energy&fuels

Article

Cite This: Energy Fuels 2019, 33, 6934−6945

pubs.acs.org/EF

Temperature-Triggered Rearrangement of Asphaltene Aggregates as Revealed by Pulsed-Field Gradient NMR

Evgeny V. Morozov,*[,†,‡,§] Pavel V. Yushmanov,[∥] and Oleg N. Martyanov[§,⊥]

[†]Institute of Chemistry and Chemical Technology, Federal Research Center "Krasnoyarsk Scientific Center SB RAS", Akademgorodok 50/24, Krasnoyarsk 660036, Russia

[‡]Kirensky Institute of Physics, Federal Research Center "Krasnoyarsk Scientific Center SB RAS", Akademgorodok 50/38, Krasnoyarsk 660036, Russia

[§]Boreskov Institute of Catalysis, Siberian Branch of Russian Academy of Sciences, Ak. Lavrentieva 5, Novosibirsk 630090, Russia

[∥]P&L Scientific Instrument Services, Box 1241, 181 24 Lidingö, Sweden

[⊥]Novosibirsk State University, Pirogova str. 2, Novosibirsk 630090, Russia

Supporting Information

ABSTRACT: The tendency of asphaltenes for aggregation followed by precipitation and deposition plays a crucial role in the petroleum industry since these processes present severe problems during the production, recovery, and processing of crude oils and fossil hydrocarbon feedstocks. The dynamics of oil asphaltene aggregates dissolved in chloroform at different concentrations varied in a wide range that was investigated at temperatures from 0 to 55 °C using the Pulsed-Field Gradient NMR technique. The components attributed to nanoaggregates and macroaggregates were successfully resolved, which allowed us to measure their diffusion coefficients. The diffusion coefficients for all types of aggregates grow as the asphaltene concentration decreases, whereas the partial weight of the aggregates increases with the increase of asphaltene concentration. The difference in diffusion behavior of the aggregates of different types was registered when passing the critical concentration range 10−20 g/L. The nano- and macroaggregates behave independently when the asphaltene concentration is higher than 20 g/L (concentrated regime), while below 20 g/L (semidiluted regime) the components related to the different types of aggregates cannot be properly resolved. It was found that regardless of the asphaltene concentration, the diffusion coefficients for nano- and macroaggregates demonstrate similar temperature behavior giving the straight lines in the Arrhenius coordinates which change their slopes when passing the temperature range 20−30 °C. The phenomenon evidences the thermally induced cleavage of noncovalent bonds with subsequent rearrangement of asphaltene aggregates that is observed for all concentration regimes covering the existence of asphaltene aggregates of all types. The data obtained are well consistent with the modern concept of asphaltene aggregate structure and fairly agree with the data obtained earlier. We believe these results will contribute essentially to a better understanding of the fundamental behavior of asphaltenes and their aggregates, providing a deep insight into aggregate transformation triggered by the temperature.

1. INTRODUCTION

Abundant worldwide production of light oil along with the depletion of conventional oil resources actually shifted the focus of the petroleum industry and technology toward processing of heavier crude oils and residues.[1] Heavy crude oils are among the most complex existing natural fluids. These feedstocks are more difficult to process, in comparison with light oils, because of the higher content of heavy constituents such as asphaltenes and resin and greater quantities of nondistillable hydrocarbons having many heteroatoms and metals.[2] The main problem when processing heavy oils lies in the inevitable deposition of heavy organic compounds. Consequently, there is a strong necessity to refine permanently pipelines, internal surface of reservoirs, and catalysts in reactors from the deposits during heavy oil production and processing.

Among the thousands of components present in crude oil,[3] asphaltenes are highlighted to be the most important group of compounds that undergo deposition during processing, refining, and transportation of heavy oil.[4] They are typically defined as a nonvolatile fraction of crude oils which are insoluble in *n*-alkanes but soluble in benzene and toluene.[5,6] This definition captures the heaviest and the most polar fraction of oil, which is composed of various molecules having a strong tendency for the destabilization and phase separation. Although asphaltenes have been extensively studied over the decades, their composition and molecular structure remain under discussion so far.[7−9] In particular, such fundamental data as molecular weight, size, shape, and molecular structure are not clearly established and still is a big challenge in the characterization of asphaltenes.[10] Usually asphaltenes are considered to be formed by a system of polycondensed aromatic rings with aliphatic chains attached to them.[9,11] They also contain some heteroatoms (nitrogen, sulfur, and oxygen) and metals in trace amounts (nickel and vanadium) in proportions depending upon the origin of the sample.[12] Based on numerous experimental findings, two main structural

Received: February 27, 2019
Revised: July 9, 2019
Published: July 10, 2019

DOI: 10.1021/acs.energyfuels.9b00600
Energy Fuels 2019, 33, 6934−6945

models have been proposed for asphaltene molecule: the "continental" (or equivalently − "island") and the "archipelago" models.[7,9,12−14] According to the continental model, the asphaltenes are considered as a condensed aromatic molecule composed of a single aromatic core substituted by some alkyl chains, whereas, in the archipelago model, the asphaltene molecule consists of several smaller aromatic cores interconnected via alkyl chains and thioether bridges. The evidence in favor of each of the models are widely presented in the literature, and in turns are used by different authors to support particular experimental data concerning aggregation behavior of asphaltenes.[15]

Aggregation of asphaltenes followed by precipitation and deposition under certain external factors, such as temperature, pressure, and chemical composition changes,[6,16−18] plays a crucial role in the petroleum industry since these processes can present severe problems during the production and recovery of crude oils as well as for processing and catalytic refining of fossil hydrocarbon feedstocks. Therefore, the formation of aggregates from the individual asphaltene molecules is an essential stage in the overall precipitation process that deserves closer consideration. Nowadays it is widely accepted that asphaltenes can aggregate even in heavily diluted solutions of "good" solvents such as toluene.[9,12] According to a simplified *one-step* concept,[19] the asphaltene molecules begin to form nanoscale (3−5 nm) aggregated structures at concentrations of 50−150 mg/L, where the upper and lower limits are defined primarily by the particular experimental techniques used for detection of the aggregated structures.[20−24] However, the existence of several aggregation stages at sufficiently lower concentration (as low as several mg/L) has been repeatedly demonstrated by various experiments.[19,25−28]

The asphaltene nanoaggregates were found to have a single stack of polycyclic aromatic hydrocarbons in the interior with alkanes on the exterior.[29,30] These nanoaggregates have limited aggregation numbers and size because of molecular architecture: the alkyl chains attached to asphaltene aromatic cores produce steric repulsion; thus, only a few (<10) molecules can aggregate, forming a structure with repulsive alkanes exposed to the outside.[9] At significantly higher concentrations (about 2−5 g/L) than those needed for nanoaggregates formation, a secondary aggregation process takes place: the clustering of nanoaggregates.[12] The concentration at which this process occurs has been referred to as the critical cluster concentration (CCC).[31,32] While the asphaltene nanoaggregates were extensively studied by numerous techniques,[20−24,29,30] the nanoaggregate clusters formation has mainly been supported by the measurements of surface tension,[33] DC-conductivity,[24,31] and oil reservoir vertical asphaltene concentration gradients.[12,34] Based on the experimental data, the cluster aggregation numbers were found to be approximately ten, and the cluster was determined to be fractal with the size range 5−10 nm.[29,32,35] As the asphaltene nanoaggregates and their clusters determine the kinetic of flocculation process upon system destabilization,[9,12] it is very important to measure accurately the dynamics of the aggregates, and to probe their structure and possible phase transitions. Despite the sufficient progress in asphaltene science over the past few decades, some questions regarding the aggregates behavior are still not resolved and not fully elucidated. For instance, it is not clear why clusters growth appears to stop at ∼5 nm, or which type of morphological change in cluster periphery is required to yield coalescence.[31,36]

A variety of techniques have been used to study asphaltene aggregates at different time and length scales: small-angle neutron scattering (SANS),[16,29,37] small-angle X-ray scattering (SAXS),[16,21,29,38] X-ray diffraction (XRD),[39,40] numerous NMR and ESR methods,[41−52] dynamic light scattering (DLS),[53,54] AC/DC-conductivity measurements and centrifugation,[24,31,36] nanofiltration,[55] high-Q ultrasonics,[22] etc.[56−58] Using these methods the different parameters were elucidated in either model asphaltene solutions or native crude oils including aggregation number, size, and shape of asphaltene aggregates. The modern NMR techniques such as pulsed-field gradient (PFG) and its high-resolution version—diffusion ordered spectroscopy (DOSY)—have been successfully applied to get important structural and dynamic information about the asphaltene aggregates via the measurements of their translational motion (self-diffusion).[46,47,59−64] The PFG NMR method is inherently sensitive to the architecture of asphaltene aggregates which determines their translational motion and interactions with each other. Using this method the aggregates size,[46,61] aggregation mechanisms,[47] the interactions between asphaltenes and naphthenic acids,[62] and the interrelation between the structure and aggregation properties of asphaltenes[63] were investigated. It should be noted that attention was mainly focused toward the dependence of aggregates size and their assumed structure on the concentration of the asphaltenes in solution or solution-to-flocculant ratio, whereas the changes in the temperature-dependent dynamics of the aggregates have been largely ignored within certain temperature ranges. However, the temperature appears to significantly affect the asphaltene aggregates structure and dynamics,[65−67] causing the phase transitions of supramolecular assemblies in model systems and native crude oils.[68]

In the present study, the dynamics of aggregates of oil asphaltene dissolved in chloroform at different concentrations above the critical nanoaggregates concentration (CNAC) was investigated within the temperature range from 0 up to 55 °C using the Pulsed-Field Gradient NMR technique. The influence of the asphaltene concentration on their diffusion coefficients was studied mainly to check the consistency of the aggregates dynamics with those present in the literature, while attention was mainly focused toward the investigation of the temperature behavior of the asphaltene diffusion coefficients. The data obtained concerning the concentration-dependent dynamics of asphaltene aggregates agree well with those reported previously. However, the temperature dependencies of diffusion coefficients demonstrate remarkable phenomena which have not been previously observed. We believe that the results of this work contribute to the understanding of the fundamental behaviors of oil asphaltene aggregates and will stimulate new experimental studies to elucidate the detailed mechanism of the thermally induced trigger responsible for asphaltene aggregates rearrangement.

2. EXPERIMENTAL SECTION

2.1. Samples Preparation. Asphaltenes used for investigation were extracted from heavy oil produced in Tatar Republic (Russia) following to ASTM method D6560-00 (Standard Test Method for Determination of Asphaltenes (Heptane Insolubles) in Crude Petroleum and Petroleum Products[69]), substituting *n*-heptane and toluene as solvents for hexane and benzene, respectively, to facilitate distillation. All solvents used were reagent-grade or higher. The real density of the separated asphaltenes measured by a helium pycnometer was 1.178 g/cm^3. The measured maximum solubility of the asphaltenes in toluene was about 20 wt %.

DOI: 10.1021/acs.energyfuels.9b00600
Energy Fuels 2019, 33, 6934−6945

For the measurements of the diffusion coefficients, the solutions of asphaltenes in chloroform were prepared. The deuterated toluene-*d8* is most commonly used for the NMR measurements of asphaltene solutions; however, some trace amount of the normal ($C_6H_5CH_3$) toluene is always presented in solution with the $-CH_3$ peak position found nearby the broad shoulder originating from the protons of aliphatic side chains of the asphaltenes. Along with other proton-containing impurities which inevitably present in the solid asphaltene powder and/or liquid solvent, this might slightly affect the registered signal attenuation curves by gaining the apparent contribution of faster diffusing components. Since the behavior of asphaltenes in the chlorine containing organic solvents is similar to that observed in aromatics[74,75] and the $CHCl_3$ proton line in the NMR spectra does not overlap the resonance signal from the asphaltene at 0.7−1.9 ppm (an example of proton NMR spectrum of asphaltene solution in $CHCl_3$ is presented in Figure S1 where the aromatic, aliphatic, and solvent NMR signals can be seen), this substitution seems reasonable.

To check the concentration effect, the series of asphaltene solutions in chloroform were prepared with the following set of concentrations: 120 g/L, 80 g/L, 40 g/L, 20 g/L, 10 g/L, 5 g/L, 1.9 g/L, and 0.5 g/L (i.e., in range of 7.45−0.03 wt %); the concentration of asphaltenes in all samples studied was much higher than those typically attributed to possible CNAC,[7,9,12,20−24] ensuring the presence of the aggregated structures in solution. To study the temperature-dependent behavior of asphaltene aggregates the samples with asphaltene concentration of 120 g/L, 40 g/L, 24 g/L, and 7 g/L were studied in the temperature range from 0 to 55 °C. The upper limit of the temperature range is defined by the boiling point of the chloroform (61 °C); near this temperature, the convection becomes very strong and the interference no longer can be suppressed by appropriate PFG NMR techniques. Measurements at temperatures lower than 0 °C are impractical, since the most vital processes for the asphaltene science occur at temperatures higher than 0−10 °C (flow of heavy oil in the pipelines, heavy oil upgrading, and others). Each sample was prepared independently by dissolving the weighed portion of asphaltene powder in the certain volume of chloroform but not via diluting the concentrated solution of asphaltenes as usual. After careful mixing and equilibration, the solution with given asphaltene concentration was poured into a 5 mm NMR tube with a sealed cap to avoid possible evaporation of the solvent.

2.2. PFG NMR Measurements. The PFG NMR experiments were carried out using a Bruker Avance III 500 MHz spectrometer equipped with a Bruker GREAT 60 gradient unit and a z-gradient probe Diff30 capable of producing high strength gradient pulses (up to 1800 G/cm) with short duration and ramp times. This allowed us to keep the gradient pulse duration reasonably short, avoiding sufficient signal loss from the heaviest (i.e., the least mobile) asphaltene aggregates as they typically have the shortest spin−spin relaxation time T_2. The pulse sequence used for the diffusion measurements was a double stimulated spin−echo (DSTE) where the gradient pulse duration (δ) and the experimental observation time (diffusion time, Δ) were kept constant at 1 and 100 ms, respectively. This pulse sequence was used to remove the potential effect of constant flows (convection) in the sample since the majority of the measurements were carried out at elevated temperatures (i.e., higher than 20 °C). The value of the pulsed field gradient (g) was varied from 0 to 400 G/cm to obtain a 100-fold signal attenuation. In all experiments 16 linear gradient steps were used to obtain the signal decay with 16 or more scans for each value of g to provide a reasonable signal-to-noise ratio. As a result, the diffusion measurements data were recorded as a pseudo-2D spectrum containing the set of 1D spectra acquired at different values of the pulsed field gradient.

The real temperature inside the probe was carefully calibrated in the range 0−60 °C at a given air flow rate using an external sensor. The gradient strength was calibrated using a known diffusion coefficient of water in a H_2O/D_2O mixture. In addition to described experiments the number of the measurements was repeated using a Bruker Avance III 600 MHz spectrometer equipped with conventional spectroscopic probes capable of producing the gradient pulses up to 50 G/cm. The diffusion coefficients were measured in a similar way using a stimulated echo pulse sequence with bipolar gradients (STEBP), and δ and Δ parameters of 4 and 100 ms, respectively. This was done to ensure that no equipment/pulse sequence-related effects were brought into measured signal attenuation decays.

2.3. Data Analysis. Generally, in a PFG NMR experiment two gradient pulses are applied with a time separation (Δ), when the probed molecules are diffusing freely in space. In the case of translational self-diffusion and a single diffusion coefficient the signal attenuates according to a well-known Stejskal−Tanner expression:[76]

$$I = I_0 \exp(-\gamma^2 g^2 \delta^2 D(\Delta - \delta/3))$$

where I is the intensity of the signal, I_0 is the signal intensity at $g = 0$ (i.e., the signal intensity obtained from the first spectrum in pseudo-2D data set), D is the self-diffusion coefficient, and γ is the gyromagnetic ratio. Thus, in the case of single diffusing species the logarithm of the normalized signal attenuation (I/I_0) versus $b = \gamma^2 g^2 \delta^2 (\Delta - \delta/3)$ results in a straight line with a slope D.

However, in the complex systems such as asphaltenes solution in chloroform, the diffusing species are neither single nor monodisperse. Due to this fact the signal attenuation decay no longer can be fitted by a single exponent. One of the first approaches employed to resolve the issue is to apply the log-normal (or stretched exponential in some cases) distribution function for the analysis of the attenuation curves.[59,62,77] This approach assumes the presence of a broad distribution of the diffusion coefficients in the system and provides mathematically correct fitting of the experimental data. Unfortunately, the broad monomodal distribution being well suitable for polymer and surfactant systems is poorly consistent with the results of numerous scattering experiments on asphaltene solutions which distinctly indicate the presence of bimodal aggregates size distribution with characteristic maxima in the range 1−3 nm and 5−7 nm.

Later this fact was evidently confirmed by DOSY NMR spectroscopy for asphaltene solution in toluene: clear separation between two families of aggregates of asphaltenes was observed for concentrations higher than 3 wt %.[46,62] Actually the attenuation curve represents a decay which can be perfectly described by a sum of several modes (either delta-functions or distribution functions) instead of a broad monomodal distribution. To process PFG NMR data in this case, an inversion of Laplace transform (ILT) must be performed. That is a classical ill-conditioned problem of resolving components of a multiexponential decay:[78] within the experimental error bar or under the condition of low signal-to-noise ratio, the solution may not be unique (i.e., several solutions may be found simultaneously which satisfactorily reproduce the original data), may not exist, and may not depend continuously on the data.

Several numerical algorithms have been implemented to solve this problem in the context of diffusion data obtained via NMR spectroscopy, including the DISCRETE and CONTIN methods,[79,80] maximum entropy,[81] CORE-family algorithms,[82] DECRA,[83] etc.[84] The natural complexity of asphaltenes solution intuitively requests employing the methods which deal with continuous distribution regardless of the number of possible modes. Following this idea a number of DOSY NMR experimental studies were carried out, and the multimodal distributions of the asphaltene diffusion coefficients have been presented.[47,63,64] Being attractive from the physical point of view, the distribution however is strongly affected by the mathematical regularization procedure and the particular method used for evaluation. For instance, the widely used Tikhonov regularization method (implemented, for example, in CONTIN) requires the application of a smoothing functional which eventually makes the resulting distribution broadened regardless of its physical width.[78] As a result, the obtained distributions are rather qualitative, while the diffusion coefficient values used for further quantitative analysis *defacto* come from the distribution peaks. For this reason, a multiexponential analysis based on a fast least-squares fitting procedure has been widely used in recent works, providing reliable results.[46,61,77] Following this approach, our signal attenuation curves were analyzed within the framework of multiexponential processing based on nonlinear least-squares fitting, assuming the presence of

DOI: 10.1021/acs.energyfuels.9b00600
Energy Fuels 2019, 33, 6934−6945

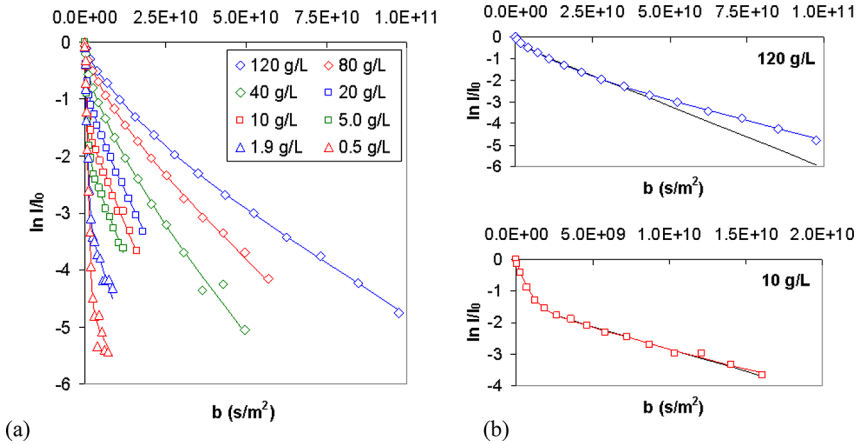

Figure 1. (a) Decays of the signal from the aliphatic hydrogens of asphaltenes dissolved in $CHCl_3$ at 20 °C for different concentrations in the range 120−0.5 g/L. The experimental data are shown as the symbols; the solid lines are the multiexponential fitting. (b) Results of two- (black line) and three-component (color line) fitting used for the simulation of signal decay for the samples with high and low concentrations of asphaltenes.

several principal components which would correspond to the peaks visible in DOSY NMR.

3. RESULTS AND DISCUSSION

3.1. Concentration-Dependent Aggregate Dynamics.

As it is demonstrated in Figure S1, the chloroform line overlaps significantly the signal of aromatic protons; therefore the diffusion measurements were carried out using the 0.0−3.0 ppm region in the spectra (Figure S2). The decays of the signal at 0.0−3.0 ppm region for different asphaltene concentrations are presented in the Figure 1. These curves obviously are not single-exponential ones (Figure 1a) as it has been repeatedly reported earlier: none of the curves measured for different concentrations can be satisfactorily fitted by a straight line. According to the data analysis strategy described above in Section 2.3, the signal attenuation curves were processed by multiexponential fitting. Previously a two-component model was proposed for data analysis.[46] This model suggests the presence of two different types of asphaltene-containing particles (bimodal distribution) formed in the solution: monomers and aggregates, yielding the fast and slow diffusion respectively that was well confirmed by numerous experimental data.[7,9,12]

Later, the two-component approach was independently validated by DOSY NMR measurements which showed the distribution of the diffusion coefficients with several (two or three, depending on the asphaltenes concentration and the samples origin) principal components.[47,63,64] Since the concentration of asphaltenes in all measured solutions was higher than that attributed to CNAC, one should expect the presence of several diffusing species such as monomers (i.e., the least aggregated structures which apparently could be dimers, trimers, and so forth), nanoaggregates, and clusters. Consequently the number of the components used for multiexponential processing was chosen to be three until the difference between the results of two- and three-component fitting became negligible, Figure 1b. Thus, in the concentration range 120−20 g/L the difference is noticeable, but at concentrations lower than 20 g/L the results of two- and three-component fitting can no longer be discerned.

The results of the fitting are presented in Figure 2. Within the concentration range from 120 g/L down to 20 g/L, three-component analysis revealed the existence of the components

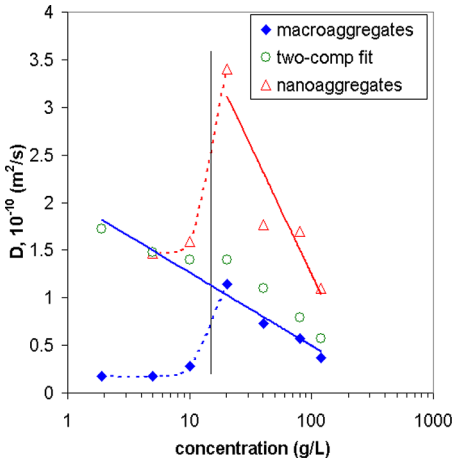

Figure 2. Concentration dependencies of diffusion coefficients extracted from two- and three-component fitting of the decays of the signal. "Two-comp fit" denotes the second component of two-component fitting; black vertical line divides the graph into 1.9−15 g/L and 15−120 g/L regions just for clarity of visual representation.

characterized by the diffusion coefficients which differ by two times or more. The first component with $D > 10^{-9}$ m^2/s (not shown in Figure 2) is attributed to the smallest species, i.e. small molecules (impurities), asphaltene molecules, and aggregates with the lowest aggregation numbers. Also some toluene and heptane molecules can be noticed in the appropriate diffusion range $(1.2–1.8) \times 10^{-9}$ m^2/s.[46,63] The second component with characteristic $D \approx 1.1 \times 10^{-10}–3.4 \times 10^{-10}$ m^2/s can be attributed to the nanoaggregates. It should be noted that some intermediate structures (microaggregates) were previously introduced into the same diffusion scale[64] together with nanoaggregates. The third and the slowest component with the characteristic $D \approx 0.3 \times 10^{-10}–1.1 \times 10^{-10}$ m^2/s is attributed to the macroaggregates (clusters); those diffusion rates agree well the data present elsewhere.[47,64]

One can see that the diffusion coefficients of nanoaggregates and clusters grow as the asphaltene concentration decreases (Figure 2), whereas the partial weight of the aggregate components increases with the increase of the asphaltene content (Figure S3). Within the concentration range 20−120 g/L, a three-component model provides reasonable diffusion

DOI: 10.1021/acs.energyfuels.9b00600
Energy Fuels 2019, 33, 6934−6945

coefficients which follow the well-established trend[47,59,85] (Figure 2, solid color lines). However, at concentrations below 20 g/L the results of two- and three-component fitting can no longer be discerned (Figure 1b) and apparent D values of the aggregates come out of their concentration trends (Figure 2, dotted color lines). It happens solely due to a mathematical reason: when the third component of the decay is physically absent (i.e., its partial weight is close to zero), the algorithm of the multicomponent analysis provides virtual values for the respective component which have no physical meaning. Consequently for this concentration range (<20 g/L) the two-component model provides more reliable data and the diffusion coefficients continue following the designated trend, Figure 2. Disappearance of the third component attributed to the asphaltene clusters below 20 g/L could indicate either that the heaviest aggregated structures are really absent or that the aggregates components can not be properly resolved.

The changes in diffusion behavior of the aggregates when passing the critical concentration range 10−20 g/L can be interpreted in two possible ways. The simplest explanation is that the size distributions of the nano- and macroaggregates overlap below 20 g/L, resulting in significant overlapping of the corresponding diffusion coefficients. In this case, the multiexponential processing is unable to resolve properly the components, giving just a characteristic value of D which is much lower than the median value of D attributed to nanoaggregates. Arguments in favor of this explanation can be found in other works where the transient regimes with overlapping distributions were clearly demonstrated.[47,63,64,86]

Another possible way to explain the phenomena observed for the 10−20 g/L range was proposed by Durand and co-workers:[47] from the microscopic point of view, if any region of the system is enriched with asphaltene macroaggregates, the others become depleted of the macroaggregates, while nanoaggregates remain free and can diffuse rather fast. As a result, upon achieving the critical concentration the component associated with macroaggregates arises with slow diffusion while that component associated with nanoaggregates begins to show much faster diffusion.

Later this explanation was re-examined within the framework of solution theory which states that asphaltenes are considered to be dissolved in the solvent, rather than being suspended as colloids. Thus, Painter and co-workers[87] confidently argue that observed differentiation in diffusion behavior is a liquid/liquid phase separation predicted to occur at asphaltene concentration near 25 g/L (in toluene). There is no evident contradiction between solution and colloidal approaches with respect to the possible explanation of the diffusion results. However, according to this explanation, the presence of the macroaggregates is not presumed below 20 g/L but the clusters formation was reported starting from 2 to 5 g/L.[7,9,12] It could mean that in the semidiluted regime (<20 g/L) the concentrations of the clusters are too small to provide the microscopic segregation (phase separation) and induce an increase in nanoaggregates mobility.

Additional information about asphaltene aggregates could have been obtained through assessment of their size. The Stokes−Einstein equation relates the diffusion coefficient D with hydrodynamic radius R_h of the moving particle: $D = kT/6\pi\eta R_h$, where k is the Boltzmann constant, T is the absolute temperature, and η is the fluid viscosity. This equation was derived by assuming that a spherical particle of colloidal dimension (much higher than that of the solvent) moves with uniform velocity in a fluid continuum and does not interact with media and other particles. Evidently it is not the case for the asphaltenes: it is well-established that they are nonspherical and actively interact with each other via different mechanisms.[47,63] Consequently the Stokes−Einstein equation provides merely a rough estimation of the aggregates size. Using the data shown in Figure 2, the R_h values 1.1−3.4 nm and 3.3−10.1 nm were obtained for nano- and macroaggregates, respectively (the concentration dependencies of R_h are present in Figure S4). As is seen, despite the erroneous nature of the approach used, these values are within the same range as those present in the literature[12,29,32,55] and in our previous studies.[38,50,51,75]

The strong concentration dependence of the diffusion coefficients of asphaltenes has been reported since the early 2000s when the first PFG NMR works[46,59−62,88] were carried out. Measured in a wide range of concentrations, the values of D were repeatedly shown to increase as the concentration decreases, being in a broad range of 0.8×10^{-10}−3.6×10^{-10} m^2/s depending on the sample's origin and particular method used of the data analysis. The results obtained in our study are within the same range: extracted from the multiexponential analysis, D values of the different components (Figure 2) match the averaged data extracted from either broad distribution[59,62,88] or simple two-component[46,61] approaches which were employed in pioneer works without proper resolution of the separate components. The approach based on DOSY NMR also confirmed the complexity of the diffusion behavior originated from the different diffusion components resolved that can be related to the different aggregation states of asphaltenes.[47,63,64,89,90] And our results are well consistent with the data obtained via DOSY. Thus, the second and third components of our multiexponential fitting match the peaks of the distribution of diffusion coefficients attributed to nano- and macroaggregates respectively, and the dynamics of the different aggregate types agree well with those revealed by DOSY NMR.[47]

The detailed discussion presented above shows that the majority of the data available in literature concern the concentration-dependent behavior of asphaltene aggregates that was rigorously studied in a wide range of concentrations, for the samples of different origin, and using numerous techniques and experimental methods. Finalizing this introductory part of the paper that is actually the basis of the main results formulated below, we can state that our data are within the conventional framework. At the same time, we systemized the overall understanding of the aggregates dynamics: in semidiluted (<20 g/L) and concentrated (>20 g/L) solutions, the asphaltenes do aggregate and form differently structured aggregates with different characteristic sizes. In concentrated solutions the different types of aggregates behave in similar way—the diffusion coefficients and the partial weights of the corresponding components have similar concentration trends. For semidiluted solutions it is reasonable to use the term "aggregates" no matter nano- or macroaggregates are presented in the system, as their dynamics cannot be properly separated via present analysis.

Based on the results obtained for concentration-dependent aggregate dynamics, the extreme concentrations of 120 g/L (high-concentration regime) and 7 g/L (semidiluted regime) seem to be the most interesting for the measurements of temperature-dependent aggregate dynamics. In addition to these two concentration values, the concentrations of 24 g/L

DOI: 10.1021/acs.energyfuels.9b00600
Energy Fuels 2019, 33, 6934−6945

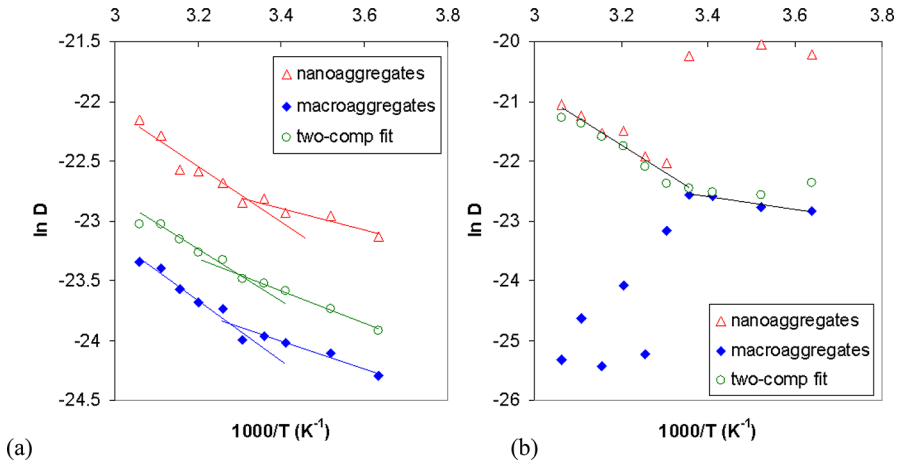

Figure 3. Temperature dependencies of diffusion coefficients extracted from two- and three-component fitting of the decays of the signal for 120 g/L (a) and 7 g/L (b) samples.

(intermediate regime) and 40 g/L (somewhere apart from the boundary) deserve to be examined.

3.2. Temperature-Dependent Aggregate Dynamics. The decays of the signal collected in the region of 0.0−3.0 ppm are shown in Figure S5a for the sample with the highest measured asphaltene concentration of 120 g/L. These decays (and all presented further) were analyzed in the same manner as those presented above (Figure 1) according to the strategy described in Section 2.3. We chose the three-component model for multiexponential processing, as the difference between two- and three-component fittings remain noticeable within the whole temperature range (Figure S5b). The similar decays were registered also for the asphaltene concentrations of 40 g/L and 24 g/L (are not shown).

Unlike the high concentration regime, the decays obtained for the semidiluted regime (7 g/L, Figure S6) were processed by either two- or three-component fitting depending on the temperature. It has been shown in Figure 1b that the two- and three-component fitting approach leads to almost the same results at concentrations lower than 20 g/L; however, the decays measured at low temperatures showed the presence of a discernible third component even in a semidiluted regime (see the plot at 0 °C, Figure S6b). Following the explanations given in the section above, this fact could be indicative of the overlapping of nano- and macroaggregates size distributions, which was suggested to explain the diffusion behavior of asphaltenes when passing the critical concentration range 10−20 g/L. This temperature variation actually is enough to affect the distributions of diffusion coefficients: while the distributions overlap at room temperature, the diffusion coefficients related to the different types of aggregates become resolved at 0 °C. Alternatively, in view of solution theory both the entropy of mixing and solubility are temperature-dependent parameters. Therefore, rather small variation of the system temperature near the boundary of the phase stability may give rise to microscopic phase separation similar to that occurred when passing the critical concentration range.[85,91,92]

The results of the fitting of the signal decays are shown in Figure 3. Following the multiexponential analysis strategy described above, three separate components with particular diffusion coefficients were clearly resolved in the decays of the 120 g/L sample. The dependences demonstrate similar temperature dynamics: the D value for every component increases with the temperature increase, and the data can be approximated with the straight line in the Arrhenius coordinates, Figure 3a (the first component related to the smallest diffusing species is not shown).

Essentially a different situation is observed in the semidiluted regime, Figure 3b. At low temperatures when the diffusion coefficient distributions can be resolved, the components associated with nano- and macroaggregates behave separately. Upon achieving the room temperature, the macroaggregates component no longer can be properly distinguished, as it was described above. As a result, D values of the macroaggregates above 25 °C become physically meaningless just being the product of the mathematical fitting procedure: they appear scattered out of any physical trend, Figure 3b. In turn, the nanoaggregates component drops down and continues the dominant trend which came from the macroaggregates component at lower temperatures. Within the temperature range 25−55 °C, both second components coming from two- and three-component fittings are close to each other and behave similarly.

The analysis of the data for the 40 g/L sample revealed a similar behavior as compared to the samples with higher concentrations (Figure 3a). In the case of the 24 g/L sample the diffusion coefficients behave somehow in between: the macroaggregates component behaves like that in Figure 3a whereas the nanoaggregates component is very scattered, dropping down like in Figure 3b upon achieving the room temperature.

The main peculiarity clearly seen in Figure 3 is the difference of the aggregates behavior below and higher than the critical temperature range 20−30 °C. One can see that with the approach to room temperature the linear trends in the Arrhenius plot change their slopes. The data are summarized in Figure 4 for all studied samples with different asphaltene concentrations: 120, 40, 24, and 7 g/L. For the simplicity of the representation, the results of two-component fitting are displayed since they reflect the behavior of nano- and macroaggregates. An unambiguous conclusion can be made that the temperature-dependent diffusion dynamics undergo a qualitative transition for the samples in a whole concentration range (in either concentrated or semidiluted regime) which covers the existence of different types of asphaltene aggregates. This transition becomes more evident at lower asphaltene concentrations, whereas at higher concentration it seems to be less pronounced; also the temperature of the transition likely

DOI: 10.1021/acs.energyfuels.9b00600
Energy Fuels 2019, 33, 6934−6945

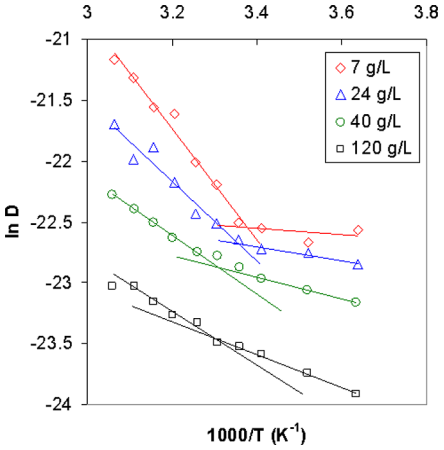

Figure 4. Temperature dependencies of diffusion coefficients extracted from two-component fitting of the decays of the signal for 120, 40, 24, and 7 g/L samples.

slightly increases with the increase of asphaltene concentration, Figure 4.

The nature of the transition observed in temperature-dependent aggregate dynamics must be thoroughly discussed. By measuring the diffusion coefficient of the species which are moving freely in space, i.e. there is no physical barriers which could restrict the translational motion, e.g. walls of the pores, etc., the translational dynamics of the molecules (or particle in general) can be probed directly. When the properties of the particle-containing medium are constant, this dynamic is solely defined by the size of the moving species and their interactions with the surrounding medium and each other; such factors as structure, composition, and surface morphology of the species affect the dynamics indirectly through the modulation of the size or effectiveness of attractive/repulsive interactions between the particles.[84] So when the particle experiences the change in its size/structure, the diffusion coefficient changes accordingly; for example, variation of the molecular mass (or equivalently—molecular size) results in characteristic change of diffusion coefficients.[85]

Temperature variation in the system could affect both the particles and the medium. When no structural changes/phase transitions happen in the system (neither with diffusing particles nor with surrounding molecules), diffusion coefficients normally follow fairly known Arrhenius type of behavior, or at least demonstrate smooth temperature dependence like those observed in the case of glass transition,[93] e.g. Vogel—Tamman—Fulcher (VTF) type of dependence. However, once either the size of the particles or interactions between them have been changed at specific temperature, the dependence experiences a nonmonotonic pattern with the break point at this particular temperature.

Results of our experiments clearly show that regardless the concentration of the asphaltenes, their aggregates do exhibit nonmonotonic temperature dynamics of diffusion coefficients. The majority of cited PFG NMR research papers dealt with the concentration as the main factor affecting the dynamics of asphaltene aggregates diluted in chloroform (benzene, toluene, or other "good" solvents), and their temperature-dependent dynamics have largely been neglected. There is only one paper[94] which examined the effect of the temperature on the asphaltene aggregates diffusion coefficients; however, no transition has been found probably because the registration temperature was too low as compared to those used in our study. On the other hand, the effect of the temperature on aggregates size has been investigated by many researchers using SANS, SAXS, DLS, photon correlation spectroscopy (PCS), etc. Generally, these studies showed the decrease of the asphaltene aggregates with the increase of the temperature;[16,95−99] however, no signs of the sharp transitions have been found until the works of Evdokimov and coauthors.[66,67,100] They performed the rheological experiments with unconventionally small temperature increments and observed noticeable structural transformations in asphaltene colloids, induced by comparatively small temperature variations within the range 26−28 °C. In their works, Evdokimov and coauthors confidently argue that this structural transformation in asphaltene aggregates is an attribute of a first-order phase transition ascribed to an endothermic breakup of noncovalent (hydrogen) bonds in analogy with polymer particles shrinkage on heating that occurred at a specific "lower critical solution temperature" (LCST).[66,67] However, this brilliant finding was not confirmed until now by other experimental techniques and has been mostly ignored by the scientific community.

Now it is well-known that LCST is observed in copolymers whose aggregation/solubility is controlled by the strength of hydrogen bonding.[101] The origin of the phase transition at LCST is mainly associated with the reorganization/destruction of the hydrogen bonding at higher temperatures, resulting in a first-order transition to compact nanoaggregates.[101−103] The strength of hydrogen bonding is a determining factor in the values of LCST, which for a wide range of polymer solutions are in a moderate interval of "physiological temperatures": 25−40 °C[67,104−107] which exactly matches the findings on asphaltene solutions. Surprisingly, measurements of diffusion coefficients of polymers subjected to coil-to-globule transition at LCST have demonstrated the temperature dynamics which is very similar to those observed in our case.[108−111]

The most important thing is that the temperature-triggered reorganization of hydrogen bonding is a general physical process which is not ultimately limited to LCST cases. For example, transformation of elongated micelles from a straight to flexible worm-like structure at transition temperatures similar to those mentioned above is caused by breaking of the intermolecular hydrogen bonds.[112] Yet the phase transitions and formation of the stable mesophases in hydrogen-bonded liquid-crystalline complexes occur near room temperature.[113] As can be seen, there are numerous examples of hydrogen bond breakup at the temperature range presented which results in structural rearrangement of complex molecules and their assemblies.

Alternatively, the solution theory of asphaltene state does not give the obvious recipes to explain the sharp kink on the temperature dependencies of diffusion coefficients, since the solubility parameters are smooth functions of the temperature. Thus, the phase separation has already occurred in the systems which are beyond the 10−20 g/L boundary, but the diffusion components of nano- and macroaggregates there (asphaltene poor and rich phases, respectively, in terms of solution theory) still behave in a similar manner. It was suggested previously[91,92] that the asphaltenes phase can be separated into a highly viscous glass-like state which experiences the glass transition at temperature similar to that in our study. It would be reasonable to suggest that both asphaltene phases undergo a glass-like transition at 20−30 °C; however, the diffusion

DOI: 10.1021/acs.energyfuels.9b00600
Energy Fuels 2019, 33, 6934−6945

dependencies do not follow the well-known VTF type which is typically seen in such cases.

In view of the concept of endothermic breakup of noncovalent bonds, it is worth discussing the possible inhibition of free movement of aggregates due to interparticle interactions which become significant at high asphaltene concentrations. It is well-known that the volume transition of nanoaggregates at LCST significantly affects the interaction potentials.[67] Thus, the breakup of noncovalent bonds facilitates interactions with surrounding molecules/particles/aggregates in polymer solutions. The interaggregate interactions are repulsive at temperatures below the LCST, typical for a hard sphere contact potential, while above LCST the potential becomes significantly attractive.[114] As a result, at temperatures above the transition the polymer aggregates attain a higher surface/interface activity, e.g. much better adsorption/retention of copolymers at solid surfaces.[115] In the case of asphaltene aggregates, the structural rearrangement similar to those occurring in polymer systems may yield the enhanced interparticle interactions.

Thermally triggered rearrangement of aggregates due to breakup of noncovalent bonds consistently explains the key features of the phenomena observed. Thus, we can see that the lower concentration, the greater the effect, Figure 4. This observation relies upon the type of aggregates involved in this temperature dependence. Breakup of noncovalent bonds and subsequent structural rearrangement affect to a much higher extent the size and dynamics of small units (nanoaggregates), whereas the macroaggregates, being the cluster composed by smaller nanoaggregates, change their size to a lesser extent. In other words, the most dramatic temperature-triggered changes occur within the basic structural units which prevail in the solution at lower concentrations. Differentiation in aggregate types also explains the shift of kink location to higher temperatures: clusters formation promotes additional noncovalent bonds in the assemblies that consequently results in a stronger bonding and higher temperature of phase transition (this effect is similar to those observed in thermoresponsive copolymers when increasing the length of monomer chain[116]).

The next observation is that the slope in diffusivity at low temperatures is lower at lower concentrations of asphaltene. It can be explained by the increase of the size/complexity of moving species together with an increase of the medium viscosity at higher concentration of asphaltene. This all leads to a decrease of particles diffusivity (according to the Stokes–Einstein equation, the diffusion coefficient is proportional to the inverse of particle size, $1/R$, and to the inverse of medium viscosity, $1/\eta$) and increase of activation energy of their translation motion. However, after the phase transition the rearranged aggregates gain interparticle interactions (as mentioned above) which are presumably stronger between the nanoaggregates as compared to those between the macroaggregates which are just the clusters of rearranged units. As can be seen, the slopes at higher temperatures are close for macroaggregates (they prevail at 120 and 40 g/L) and increases when the partial weight of nanoaggregates increases (24 and 7 g/L).

Taking into account all these considerations, it is possible to conclude that the mechanism proposed is strongly supported both by the results of complementary technique (rheological measurements performed earlier by Evdokimov and co-workers) and by multiple examples of hydrogen bond breakup at a similar temperature range in diverse polymer and supramolecular systems (with additional evidence coming from the temperature dynamics of diffusion coefficients of polymers subjected to the coil-to-globule transition at LCST). Indeed, polar and hydrogen bond interactions between the different functional groups presented in asphaltene aggregates, i.e. hydroxyls, carboxylic acids, aromatic nitrogen moieties, etc., play an important role in aggregate dynamics.[117−119] However, for a long time this role has been seriously underestimated when building the model of asphaltene aggregates structure. Recently, a new "supramolecular assembly" concept appears which states that $\pi-\pi$ stacking is not the only interaction responsible for the asphaltene aggregates structure, while acid–base interaction, *hydrogen bonding*, metal coordination, and hydrophobic pockets contribute all into the supramolecular assembly of aggregates.[119] In view of this concept, our finding is a missing link which allows extension of the general properties of supramolecular assemblies to the asphaltene aggregates since it is shown that the aggregates undergo similar temperature-triggered transitions as those colloids thoroughly studied before. Also the results explicitly show the crucial role of the temperature in asphaltene aggregate dynamics, which is as much important as the concentration of the asphaltenes. It is obvious that further experimental work is still required to elucidate all the details of the thermally induced structural rearrangement of the asphaltene aggregates.

4. CONCLUSIONS

In the present study, the dynamics of aggregates of oil asphaltenes dissolved in chloroform at different concentrations varied in a wide range was investigated at temperatures from 0 to 55 °C using a Pulsed-Field Gradient NMR technique. Within the concentration range from 120 g/L down to 20 g/L, three components of diffusion coefficients distribution were resolved which correspond to small molecules (asphaltene monomers and possible aggregates with the lowest aggregation numbers), nanoaggregates, and macroaggregates (clusters), respectively. The diffusion coefficients of all components grow as the asphaltene concentration decreases, whereas the partial weight of the components attributed to the aggregated structures increases with the increase of the asphaltene concentration.

The difference in diffusion behavior of the aggregates was registered when passing the critical concentration range 10–20 g/L. The nano- and macroaggregates behave independently in case the asphaltene concentrations are higher than 20 g/L (concentrated regime), while below 20 g/L (semidiluted regime) the components related to the different types of aggregates cannot be properly resolved. The systematic study of the concentration dependence of the diffusion coefficients are well consistent with the recognized model of the asphaltene state in solution and fairly agree with the results published earlier, confirming the validity of the applied experimental approach.

Attention was focused toward the temperature behavior of the asphaltene diffusion coefficients. In a concentrated (20–120 g/L) regime, the diffusion components corresponding to nano- and macroaggregates were successfully resolved in the whole temperature range of 0–55 °C. In the semidiluted (below 20 g/L) regime, these components became resolved below room temperature despite the fact that the distributions of their diffusion coefficients overlap at higher temperatures. Regardless the regime, the diffusion coefficients related to the nano- and macroaggregates demonstrate similar temperature

DOI: 10.1021/acs.energyfuels.9b00600
Energy Fuels 2019, 33, 6934–6945

behavior, increasing with temperature and giving straight lines in the Arrhenius coordinates. However, the temperature dependences demonstrate a sharp kink which differentiates the diffusion behavior of the asphaltene aggregates below and higher than the critical temperature range 20−30 °C.

The revealed phenomenon is observed in the whole range of asphaltenes concentration, which covers the existence of asphaltene aggregates of different types. This fact points to the thermally induced structural rearrangements of asphaltene aggregates probably originated from thermally induced break-up of hydrogen bonds. This remarkable phenomenon was not studied previously via PFG NMR and is revealed for the first time. However, it fits well the recognized picture of asphaltenes behavior and supported by many other experimental data, including those obtained via precise rheology study of aggregated systems using small temperature increments. The results obtained in our work improve the overall understanding of asphaltene aggregates behavior in solution, providing deeper insight into aggregates transformation triggered by the temperature effect. Actually, the phenomenon revealed can be considered as a missing link within the modern concept of asphaltenes structure and their behavior under certain external conditions. The temperatures within the range from 20 to 30 °C are very important for many industrial processes giving an additional significance to the phenomenon observed. We believe that the results of our work give a noticeable contribution to the better understanding of the fundamental behavior of asphaltenes and will also stimulate further experimental studies to elucidate the detailed mechanism of the structural transformation of the asphaltene aggregates in real systems.

■ ASSOCIATED CONTENT

Supporting Information

The Supporting Information is available free of charge on the ACS Publications website at DOI: 10.1021/acs.energyfuels.9b00600.

> Proton NMR spectra of the asphaltene solution in $CHCl_3$, concentration dependences of the partial weights of the diffusion components, concentration dependencies of the hydrodynamic radius of asphaltene aggregates, temperature dependences of the signal attenuation decays (PDF)

■ AUTHOR INFORMATION

Corresponding Author

*E-mail: morozovev@iph.krasn.ru; morozov_if@mail.ru.

ORCID

Evgeny V. Morozov: 0000-0003-1561-3937

Oleg N. Martyanov: 0000-0001-9999-8680

Notes

The authors declare no competing financial interest.

■ ACKNOWLEDGMENTS

This research was performed using the equipment of Krasnoyarsk Regional Research Equipment Centre of Siberian Branch of Russian Academy of Sciences with the financial support of Russian Science Foundation (Project No. 15-19-00119).

■ REFERENCES

(1) Shah, A.; Fishwick, R.; Wood, J.; Leeke, G.; Rigby, S.; Greaves, M. A review of novel techniques for heavy oil and bitumen extraction and upgrading. *Energy Environ. Sci.* **2010**, *3*, 700−714.

(2) Trejo, F.; Centeno, G.; Ancheyta, J. Precipitation, fractionation and characterization of asphaltenes from heavy and light crude oils. *Fuel* **2004**, *83*, 2169−2175.

(3) Hughey, C. A.; Rodgers, R. P.; Marshall, A. G. Resolution of 11.000 compositionally distinct components in a single electrospray ionization Fourier transform ion cyclotron resonance mass spectrum of crude oil. *Anal. Chem.* **2002**, *74*, 4145−9.

(4) Leontaritis, K. J.; Mansoori, G. A. Asphaltene Deposition: A Survey of Field Experiences and Research Approaches. *J. Pet. Sci. Eng.* **1988**, *1*, 229−239.

(5) Wiehe, I. A.; Liang, K. S. Asphaltenes, Resins, and Other Petroleum Macromolecules. *Fluid Phase Equilib.* **1996**, *117*, 201−210.

(6) Mullins, O. C.; Sheu, E. Y.; Hammami, A.; Marshall, A. G. *Asphaltenes, Heavy Oils, and Petroleomics*; Springer: New York, 2007.

(7) Mullins, O. C. *Energy Fuels* **2010**, *24*, 2179−2207.

(8) Li, D. D.; Greenfield, M. L. High internal energies of proposed asphaltene structures. *Energy Fuels* **2011**, *25*, 3698−3705.

(9) Mullins, O. C.; Sabbah, H.; Eyssautier, J. l.; Pomerantz, A. E.; Barré, L.; Andrews, A. B.; Ruiz-Morales, Y.; Mostowfi, F.; McFarlane, R.; Goual, L.; et al. Advances in asphaltene science and the Yen-Mullins model. *Energy Fuels* **2012**, *26*, 3986−4003.

(10) Sjöblom, J.; Simon, S.; Xu, Z. Model molecules mimicking asphaltenes. *Adv. Colloid Interface Sci.* **2015**, *218*, 1−16.

(11) Groenzin, H.; Mullins, O. C. Molecular Size and Structure of Asphaltenes from Various Sources. *Energy Fuels* **2000**, *14*, 677−684.

(12) Mullins, O. C. The asphaltenes. *Annu. Rev. Anal. Chem.* **2011**, *4*, 393−418.

(13) Chacón-Patiño, M. L.; Rowland, S. M.; Rodgers, R. P. Advances in Asphaltene Petroleomics. Part 3. Dominance of Island or Archipelago Structural Motif Is Sample Dependent. *Energy Fuels* **2018**, *32* (9), 9106−9120.

(14) Bava, Y. B.; Geronés, M.; Buceta, D.; Rodríguez, D. de la I.; López-Quintela, M. A.; Erben, M. F. Elucidation of the Average Molecular Structure of Argentinian Asphaltenes. *Energy Fuels* **2019**, *33* (4), 2950−2960.

(15) Hosseini-Dastgerdi, Z.; Tabatabaei-Nejad, S. A. R.; Khodapanah, E.; Sahraei, E. A comprehensive study on mechanism of formation and techniques to diagnose asphaltene structure; molecular and aggregates: a review. *Asia-Pac. J. Chem. Eng.* **2015**, *10*, 1−14.

(16) Espinat, D.; Fenistein, D.; Barre, L.; Frot, D.; Briolant, Y. Effects of Temperature and Pressure on Asphaltenes Agglomeration in Toluene. A Light, X-ray, and Neutron Scattering Investigation. *Energy Fuels* **2004**, *18*, 1243−1249.

(17) Buenrostro-Gonzalez, E.; Lira-Galeana, C.; Gil-Villegas, A.; Wu, J. Z. Asphaltene precipitation in crude oils: Theory and experiments. *AIChE J.* **2004**, *50*, 2552−2570.

(18) Maqbool, T.; Srikiratiwong, P.; Fogler, H. S. Effect of Temperature on the Precipitation Kinetics of Asphaltenes. *Energy Fuels* **2011**, *25*, 694−700.

(19) Evdokimov, I. N.; Fesan, A. A. Multi-step formation of asphaltene colloids in dilute solutions. *Colloids Surf., A* **2016**, *492*, 170−180.

(20) Fenistein, D.; Barre, L.; Espinat, D.; Livet, A.; Roux, J.-N.; Scarcella, M. Viscosimetric and neutron scattering study of asphaltene aggregates in mixed toluene/heptane solvents. *Langmuir* **1998**, *14*, 1013−20.

(21) Fenistein, D.; Barre, L. Experimental measurement of the mass distribution of petroleum asphaltene aggregates using ultracentrifugation and small-angle X-ray scattering. *Fuel* **2001**, *80*, 283−287.

(22) Andreatta, G.; Bostrom, N.; Mullins, O. C. High-Q ultrasonic determination of the critical nanoaggregate concentration of asphaltenes and the critical micelle concentration of standard surfactants. *Langmuir* **2005**, *21*, 2728−2736.

DOI: 10.1021/acs.energyfuels.9b00600
Energy Fuels 2019, 33, 6934−6945

(23) Goncalves, S.; Castillo, J.; Fernandez, A.; Hung, J. Absorbance and fluorescence spectroscopy on the aggregation of asphaltene-toluene solutions. *Fuel* **2004**, *83*, 1823−1828.
(24) Zeng, H.; Song, Y. Q.; Johnson, D. L.; Mullins, O. C. Critical nanoaggregate concentration of asphaltenes by low frequency conductivity. *Energy Fuels* **2009**, *23*, 1201−1208.
(25) Yokota, T.; Scriven, F.; Montgomery, D. S.; Strausz, O. P. Absorption and emission spectra of Athabasca asphaltene in the visible and near ultraviolet regions. *Fuel* **1986**, *65*, 1142−1149.
(26) Zhang, Y.; Takanohashi, T.; Sato, S.; Kondo, T.; Saito, I.; Tanaka, R. Dissolution and dilution of asphaltenes in organic solvents. *Energy Fuels* **2003**, *17*, 101−106.
(27) Juyal, P.; Merino-Garcia, D.; Andersen, S. I. Effect on molecular interactions of chemical alteration of petroleum asphaltenes. *Energy Fuels* **2005**, *19*, 1272−1281.
(28) McKenna, A. M.; Donald, L. J.; Fitzsimmons, J. F.; Juyal, P.; Spicer, V.; Standing, K. G.; Marshall, A. G.; Rodgers, R. P. Heavy petroleum composition. 3. Asphaltene aggregation. *Energy Fuels* **2013**, *27*, 1246−1256.
(29) Eyssautier, J.; Levitz, P.; Espinat, D.; Jestin, J.; Gummel, J.; Grillo, I.; Barré, L. Insight into asphaltene nanoaggregate structure inferred by small angle neutron and X-ray scattering. *J. Phys. Chem. B* **2011**, *115*, 6827−6837.
(30) Barré, L.; Jestin, J.; Morisset, A.; Palermo, T.; Simon, S. Relation between nanoscale structure of asphaltene aggregates and their macroscopic solution properties. *Oil Gas Sci. Technol.* **2009**, *64*, 617−628.
(31) Goual, L.; Sedghi, M.; Zeng, H.; Mostowfi, F.; McFarlane, R.; Mullins, O. C. On the Formation and Properties of Asphaltene Nanoaggregates and Clusters by DC-Conductivity and Centrifugation. *Fuel* **2011**, *90*, 2480−2490.
(32) Hoepfner, M. P.; Fogler, H. S. Multiscale Scattering Investigations of Asphaltene Cluster Breakup, Nanoaggregate Dissociation, and Molecular Ordering. *Langmuir* **2013**, *29*, 15423−15432.
(33) Rogel, E.; León, O.; Torres, G.; Espidel, J. Aggregation of Asphaltenes in Organic Solvents Using Surface Tension Measurements. *Fuel* **2000**, *79*, 1389−1394.
(34) Mullins, O. C.; Zuo, J. Y.; Seifert, D.; Zeybek, M. Clusters of Asphaltene Nanoaggregates Observed in Oil Reservoirs. *Energy Fuels* **2013**, *27*, 1752−1761.
(35) Hoepfner, M. P.; FáVero, C. V. B.; Haji-Akbari, N.; Fogler, H. S. The Fractal Aggregation of Asphaltenes. *Langmuir* **2013**, *29*, 8799−8808.
(36) Goual, L.; Sedghi, M.; Mostowfi, F.; McFarlane, R.; Pomerantz, A. E.; Saraji, S.; Mullins, O. C. Cluster of Asphaltene Nanoaggregates by DC Conductivity and Centrifugation. *Energy Fuels* **2014**, *28*, 5002−5013.
(37) Sheu, E. Y. Small angle scattering and asphaltenes. *J. Phys.: Condens. Matter* **2006**, *18*, S2485−S2498.
(38) Larichev, Yu. V.; Martyanov, O. N. The dynamics of asphaltene aggregates in heavy crude oils on a nanometer scale studied via small-angle X-ray scattering in situ. *J. Pet. Sci. Eng.* **2018**, *165*, 575−580.
(39) Andersen, S. I.; Jensen, J. O.; Speight, J. G. X-ray Diffraction of Subfractions of Petroleum Asphaltenes. *Energy Fuels* **2005**, *19*, 2371−2377.
(40) Tanaka, R.; Sato, E.; Hunt, J. E.; Winans, R. E.; Sato, S.; Takanohashi, T. Characterization of asphaltene aggregates using X-ray diffraction and small-angle X-ray scattering. *Energy Fuels* **2004**, *18*, 1118−1125.
(41) Martyanov, O. N.; Larichev, Yu. V.; Morozov, E. V.; Trukhan, S. N.; Kazarian, S. G. Development and application of advanced methods *in situ* for studying the stability and physicochemical evolution of oil systems. *Russ. Chem. Rev.* **2017**, *86*, 999−1023.
(42) Majumdar, R. D.; Gerken, M.; Mikula, R.; Hazendonk, P. Validation of the Yen-Mullins model of athabasca oil-sands asphaltenes using solution-state 1H NMR relaxation and 2D HSQC spectroscopy. *Energy Fuels* **2013**, *27*, 6528−6537.
(43) Majumdar, R. D.; Montina, T.; Mullins, O. C.; Gerken, M.; Hazendonk, P. Insights into asphaltene aggregate structure using ultrafast MAS solid-state 1H NMR spectroscopy. *Fuel* **2017**, *193*, 359−368.
(44) Prunelet, A.; Fleury, M.; Cohen-Addad, J.-P. Detection of asphaltene flocculation using NMR relaxometry. *C. R. Chim.* **2004**, *7*, 283−289.
(45) Zielinski, L.; Saha, I.; Freed, D. E.; Hurlimann, M. D.; Liu, Y. Probing Asphaltene Aggregation in Native Crude Oils with Low-Field NMR. *Langmuir* **2010**, *26*, 5014−5021.
(46) Kawashima, H.; Takanohashi, T.; Iino, M.; Matsukawa, S. Determining Asphaltene Aggregation in Solution from Diffusion Coefficients As Determined by Pulsed-Field Gradient Spin-Echo 1H NMR. *Energy Fuels* **2008**, *22*, 3989−3993.
(47) Durand, E.; Clemancey, M.; Lancelin, J.-M.; Verstraete, J.; Espinat, D.; Quoineaud, A.-A. Aggregation states of asphaltenes: Evidence of two chemical behaviors by 1H diffusion-ordered spectroscopy nuclear magnetic resonance. *J. Phys. Chem. C* **2009**, *113*, 16266−16276.
(48) Gabrienko, A. A.; Morozov, E. V.; Subramani, V.; Martyanov, O. N.; Kazarian, S. G. Chemical Visualization of Asphaltenes Aggregation Processes Studied in Situ with ATR-FTIR Spectroscopic Imaging and NMR Imaging. *J. Phys. Chem. C* **2015**, *119*, 2646−2660.
(49) Morozov, E. V.; Martyanov, O. N. Reversibility of asphaltene aggregation as revealed by Magnetic Resonance Imaging in situ. *Energy Fuels* **2017**, *31*, 10639−10647.
(50) Trukhan, S. N.; Yudanov, V. F.; Gabrienko, A. A.; Subramani, V.; Kazarian, S. G.; Martyanov, O. N. In-situ ESR Study of Molecular Dynamics of Asphaltenes at Elevated Temperature and Pressure. *Energy Fuels* **2014**, *28*, 6315−6321.
(51) Trukhan, S. N.; Kazarian, S. G.; Martyanov, O. N. Electron spin resonance of slowly rotating vanadyls - effective tool to quantify the sizes of asphaltenes in situ. *Energy Fuels* **2017**, *31*, 387−394.
(52) Gafurov, M. R.; Volodin, M. A.; Rodionov, A. A.; Sorokina, A. T.; Dolomatov, M. Y.; Petrov, A. V.; Vakhin, A. V.; Mamin, G. V.; Orlinskii, S. B. EPR study of spectra transformations of the intrinsic vanadyl-porphyrin complexes in heavy crude oils with temperature to probe the asphaltenes' aggregation. *J. Pet. Sci. Eng.* **2018**, *166*, 363−368.
(53) Hashmi, S. M.; Firoozabadi, A. Effect of dispersant on asphaltene suspension dynamics: Aggregation and sedimentation. *J. Phys. Chem. B* **2010**, *114*, 15780−15788.
(54) Eyssautier, J.; Frot, D.; Barré, L. Structure and dynamic properties of colloidal asphaltene aggregates. *Langmuir* **2012**, *28*, 11997−12004.
(55) Yarranton, H. W.; Ortiz, D. P.; Barrera, D. M.; Baydak, E. N.; Barré, L.; Frot, D.; Eyssautier, J.; Zeng, H.; Xu, Z.; Dechaine, G.; Becerra, M.; Shaw, J. M.; McKenna, A. M.; Mapolelo, M. M.; Bohne, C.; Yang, Z.; Oake, J. On the size distribution of self-associated asphaltenes. *Energy Fuels* **2013**, *27*, 5083−5106.
(56) Andersen, S. I.; Birdi, K. S. Aggregation of Asphaltenes as Determined by Calorimetry. *J. Colloid Interface Sci.* **1991**, *142*, 497−502.
(57) Wattana, P.; Wojciechowski, D. J.; Bolaños, G.; Fogler, H. S. Study of Asphaltene Precipitation Using Refractive Index Measurement. *Pet. Sci. Technol.* **2003**, *21*, 591−613.
(58) Ghosh, A. K.; Chaudhuri, P.; Kumar, B.; Panja, S. S. Review on aggregation of asphaltene vis-a-vis spectroscopic studies. *Fuel* **2016**, *185*, 541−554.
(59) Ostlund, J.-A.; Andersson, S.-I.; Nyden, M. Studies of asphaltenes by the use of pulsed-field gradient spin-echo NMR. *Fuel* **2001**, *80*, 1529−1533.
(60) Norinaga, K.; Wargardalam, V. J.; Takasugi, S.; Iino, M.; Matsukawa, S. Measurement of Self-Diffusion Coefficient of Asphaltene in Pyridine by Pulsed Field Gradient Spin-Echo 1H NMR. *Energy Fuels* **2001**, *15*, 1317−1318.
(61) Lisitza, N. V.; Freed, D. E.; Sen, P. N.; Song, Y.-Q. Study of Asphaltene Nanoaggregation by Nuclear Magnetic Resonance (NMR). *Energy Fuels* **2009**, *23*, 1189−1193.

DOI: 10.1021/acs.energyfuels.9b00600
Energy Fuels 2019, 33, 6934−6945

(62) Ostlund, J.-A.; Nyden, M.; Auflem, I. H.; Sjoblom, J. Interactions between Asphaltenes and Naphthenic Acids. *Energy Fuels* **2003**, *17*, 113−119.
(63) Durand, E.; Clemancey, M.; Lancelin, J.-M.; Verstraete, J.; Espinat, D.; Quoineaud, A.-A. Effect of Chemical Composition on Asphaltenes Aggregation. *Energy Fuels* **2010**, *24*, 1051−1062.
(64) Oliveira, E. C. S.; Neto, A. C.; Júnior, V. L.; Castro, E. V. R.; Menezes, S. M. C. Study of Brazilian asphaltene aggregation by Nuclear Magnetic Resonance spectroscopy. *Fuel* **2014**, *117*, 146−151.
(65) Mehranfar, M.; Gaikwad, R.; Das, S.; Mitra, S. K.; Thundat, T. Effect of Temperature on Morphologies of Evaporation-Triggered Asphaltene Nanoaggregates. *Langmuir* **2014**, *30*, 800−804.
(66) Evdokimov, I. N.; Eliseev, N. Yu.; Eliseev, D. Yu. Rheological evidence of structural phase transitions in asphaltene-containing petroleum fluids. *J. Pet. Sci. Eng.* **2001**, *30*, 199−211.
(67) Evdokimov, I. N.; Eliseev, N. Yu. Thermally Responsive Properties of Asphaltene Dispersions. *Energy Fuels* **2006**, *20*, 682−687.
(68) Ganeeva, Yu. M.; Yusupova, T. N.; Romanov, G. V. Asphaltene nano-aggregates: structure, phase transitions and effect on petroleum systems. *Russ. Chem. Rev.* **2011**, *80*, 993−1008.
(69) ASTM D6560, Standard Test Method for Determination of Asphaltenes (Heptane Insolubles) in Crude Petroleum and Petroleum Products; ASTM International: West Conshohocken, PA, 2012. http://www.astm.org/Standards/D6560.htm.
(70) Gabrienko, A. A.; Subramani, V.; Martyanov, O. N.; Kazarian, S. G. Correlation between Asphaltene Stability in n-Heptane and Crude Oil Composition Revealed with In Situ Chemical Imaging. *Adsorpt. Sci. Technol.* **2014**, *32*, 243−256.
(71) Morozov, E. V.; Trukhan, S. N.; Larichev, Yu. V.; Subramani, V.; Gabrienko, A. A.; Kazarian, S. G.; Martyanov, O. N. In-situ studies of crude oil stability and direct visualization of asphaltenes aggregation processes via some spectroscopy techniques. *Proceedings of 248th National Meeting of the American Chemical Society*. San Francisco, CA, 2014; p 531.
(72) Gabrienko, A. A.; Martyanov, O. N.; Kazarian, S. G. Effect of Temperature and Composition on the Stability of Crude Oil Blends Studied with Chemical Imaging in Situ. *Energy Fuels* **2015**, *29*, 7114−7123.
(73) Morozov, E. V.; Martyanov, O. N. Probing Flocculant-Induced Asphaltene Precipitation Via NMR Imaging: From Model Toluene-Asphaltene Systems To Natural Crude Oils. *Appl. Magn. Reson.* **2016**, *47*, 223−235.
(74) Oh, K.; Ring, T. A.; Deo, M. D. Asphaltene aggregation in organic solvents. *J. Colloid Interface Sci.* **2004**, *271*, 212−219.
(75) Larichev, Yu. V.; Nartova, A. V.; Martyanov, O. N. The influence of different organic solvents on the size and shape of asphaltene aggregates studied via small-angle X-ray scattering and scanning tunneling microscopy. *Adsorpt. Sci. Technol.* **2016**, *34*, 244−257.
(76) Stejskal, E. O.; Tanner, J. E. Spin diffusion measurements: spin echoes in the presence of a time - dependent field gradient. *J. Chem. Phys.* **1965**, *42*, 288−292.
(77) Ostlund, J.-A.; Nyden, M.; Stilbs, P. Component-Resolved Diffusion in Multicomponent Mixtures. A Case Study of High-Field PGSE-NMR Self-Diffusion Measurements in Asphaltene/Naphthenic Acid/Solvent Systems. *Energy Fuels* **2004**, *18*, 531−538.
(78) Istratov, A. A.; Vyvenko, O. F. Exponential analysis in physical phenomena. *Rev. Sci. Instrum.* **1999**, *70*, 1233−1257.
(79) Provencher, S. W. An eigenfunction expansion method for the analysis of exponential decay curves. *J. Chem. Phys.* **1976**, *64*, 2772−2777.
(80) Provencher, S. W. CONTIN: A general purpose constrained regularization program for inverting noisy linear algebraic and integral equations. *Comput. Phys. Commun.* **1982**, *27*, 229−242.
(81) Delsuc, M. A.; Malliavin, T. E. Maximum entropy processing of DOSY NMR spectra. *Anal. Chem.* **1998**, *70*, 2146−2148.
(82) Stilbs, P.; Paulsen, K.; Griffiths, P. C. Global Least-Squares Analysis of Large, Correlated Spectral Data Sets: Application to Component-Resolved FT-PGSE NMR Spectroscopy. *J. Phys. Chem.* **1996**, *100*, 8180−8189.
(83) Antalek, B. Using pulsed gradient spin echo NMR for chemical mixture analysis: How to obtain optimum results. *Concepts Magn. Reson.* **2002**, *14*, 225−258.
(84) Pagès, G.; Gilard, V.; Martino, R.; Malet-Martino, M. Pulsed-field gradient nuclear magnetic resonance measurements (PFG NMR) for diffusion ordered spectroscopy (DOSY) mapping. *Analyst* **2017**, *142*, 3771.
(85) Auge, S.; Schmit, P.-O.; Crutchfield, C. A.; Islam, M. T.; Harris, D. J.; Durand, E.; Clemancey, M.; Quoineaud, A.-A. NMR Measure of Translational Diffusion and Fractal Dimension. *J. Phys. Chem. B* **2009**, *113*, 1914−1918.
(86) Vorapalawut, N.; Nicot, B.; Louis-Joseph, A.; Korb, J.-P. Probing Dynamics and Interaction of Maltenes with Asphaltene Aggregates in Crude Oils by Multiscale NMR. *Energy Fuels* **2015**, *29*, 4911−4920.
(87) Painter, P.; Veytsman, B.; Youtcheff, J. Asphaltene Aggregation and Solubility. *Energy Fuels* **2015**, *29*, 2120−2133.
(88) Ostlund, J.-A.; Wattana, P.; Nydén, M.; Fogler, H. S. Characterization of fractionated asphaltenes by UV−vis and NMR self-diffusion spectroscopy. *J. Colloid Interface Sci.* **2004**, *271*, 372−380.
(89) Durand, E.; Clemancey, M.; Quoineaud, A.-A.; Verstraete, J.; Espinat, D.; Lancelin, J.-M. 1H Diffusion-Ordered Spectroscopy (DOSY) Nuclear Magnetic Resonance (NMR) as a Powerful Tool for the Analysis of Hydrocarbon Mixtures and Asphaltenes. *Energy Fuels* **2008**, *22*, 2604−2610.
(90) Júnior, L. S. C.; Menezes, S. M. C.; Honorato, H. A.; Oliveira, M. C. K.; Marques, L. C. C. Diffusion-Ordered Spectroscopy Nuclear Magnetic Resonance as an Alternative Technique to Improve Asphaltene Characterization. *Energy Fuels* **2018**, *32*, 2793−2800.
(91) Sirota, E. B. Physical Structure of Asphaltenes. *Energy Fuels* **2005**, *19*, 1290−1296.
(92) Sirota, E. B.; Lin, M. Y. *Energy Fuels* **2007**, *21*, 2809−2815.
(93) Holz, M.; Heil, S. R.; Sacco, A. Temperature-dependent self-diffusion coefficients of water and six selected molecular liquids for calibration in accurate 1H NMR PFG measurements. *Phys. Chem. Chem. Phys.* **2000**, *2*, 4740−4742.
(94) Ostlund, J.-A.; Lofroth, J.-E.; Holmberg, K.; Nyden, M. Flocculation Behavior of Asphaltenes in Solvent/Nonsolvent Systems. *J. Colloid Interface Sci.* **2002**, *253*, 150−158.
(95) Mansur, C. R.; Melo, A. R.; Lucas, E. F. Determination of asphaltene particle size: influence of flocculant, additive, and temperature. *Energy Fuels* **2012**, *26*, 4988−4994.
(96) Torkaman, M.; Bahrami, M.; Dehghani, M. Influence of Temperature on Aggregation and Stability of Asphaltenes. I. Perikinetic Aggregation. *Energy Fuels* **2017**, *31*, 11169−11180.
(97) Torkaman, M.; Bahrami, M.; Dehghani, M. Influence of Temperature on Aggregation and Stability of Asphaltenes: II. Orthokinetic Aggregation. *Energy Fuels* **2018**, *32*, 6144−6154.
(98) Zhang, S.; Zhang, L.; Lu, X.; Shi, C.; Tang, T.; Wang, X.; Huang, Q.; Zeng, H. Adsorption kinetics of asphaltenes at oil/water interface: Effects of concentration and temperature. *Fuel* **2018**, *212*, 387−394.
(99) Hemmati-Sarapardeh, A.; Dabir, B.; Ahmadi, M.; Mohammadi, A. H.; Husein, M. M. Toward mechanistic understanding of asphaltene aggregation behavior in toluene: The roles of asphaltene structure, aging time, temperature, and ultrasonic radiation. *J. Mol. Liq.* **2018**, *264*, 410−424.
(100) Evdokimov, I. N. T-C Phase Diagram of Asphaltenes in Solutions. *Pet. Sci. Technol.* **2007**, *25*, 5−17.
(101) Zhang, J. *Switchable and Responsive Surfaces and Materials for Biomedical Applications*; Woodhead Publishing: 2015; 324 pages.
(102) Deshmukh, S.; Mooney, D. A.; McDermott, T.; Kulkarni, S.; MacElroy, J. M D. Molecular modeling of thermo-responsive hydrogels: observation of lower critical solution temperature. *Soft Matter* **2009**, *5*, 1514−1521.

DOI: 10.1021/acs.energyfuels.9b00600
Energy Fuels 2019, 33, 6934−6945

(103) Alaghemandi, M.; Spohr, E. Molecular Dynamics Investigation of the Thermo-Responsive Polymer Poly(N-isopropylacrylamide). *Macromol. Theory Simul.* **2012**, *21*, 106−112.
(104) Fujishige, S.; Kubota, K.; Ando, I. Phase transition of aqueous solutions of poly(N-isopropylacrylamide) and poly(N-isopropylmethacrylamide). *J. Phys. Chem.* **1989**, *93*, 3311−3313.
(105) Schild, H.; Tirrell, D. A. Microcalorimetric detection of lower critical solution temperatures in aqueous polymer solutions. *J. Phys. Chem.* **1990**, *94*, 4352−4356.
(106) Dai, S.; Tam, K. C. Isothermal Titration Calorimetric Studies on the Temperature Dependence of Binding Interactions between Poly(propylene glycol)s and Sodium Dodecyl Sulfate. *Langmuir* **2004**, *20* (6), 2177−2183.
(107) Ahn, S.; Kasi, R. M.; Kim, S.-C.; Sharma, N.; Zhou, Y. Stimuli-responsive polymer gels. *Soft Matter* **2008**, *4*, 1151−1157.
(108) Larsson, A.; Kuckling, D.; Schonhoff, M. 1H NMR of thermoreversible polymers in solution and at interfaces: the influence of charged groups on the phase transition. *Colloids Surf., A* **2001**, *190*, 185−192.
(109) Rusu, M.; Wohlrab, S.; Kuckling, D.; Mohwald, H.; Schonhoff, M. Coil-to-Globule Transition of PNIPAM Graft Copolymers with Charged Side Chains: A 1H and 2H NMR and Spin Relaxation Study. *Macromolecules* **2006**, *39*, 7358−7363.
(110) Yushmanov, P. V.; Furo, I.; Iliopoulos, I. Kinetics of Demixing and Remixing Transitions in Aqueous Solutions of Poly(N-isopropylacrylamide): A Temperature-Jump 1H NMR Study. *Macromol. Chem. Phys.* **2006**, *207*, 1972−1979.
(111) Schweizerhof, S.; Demco, D. E.; Mourran, A.; Fechete, R.; Möller, M. Polymers Diffusivity Encoded by Stimuli-Induced Phase Transition: Theory and Application to Poly(N-Isopropylacrylamide) with Hydrophilic and Hydrophobic End Groups. *Macromol. Chem. Phys.* **2018**, *219*, 1700587.
(112) Morita, C.; Imura, Y.; Ogawa, T.; Kurata, H.; Kawai, T. Thermal-Sensitive Viscosity Transition of Elongated Micelles Induced by Breaking Intermolecular Hydrogen Bonding of Amide Groups. *Langmuir* **2013**, *29*, 5450−5456.
(113) Kato, T.; Fukumasa, M.; Frechet, J. M. J. Supramolecular Liquid-Crystalline Complexes Exhibiting Room-Temperature Mesophases and Electrooptic Effects. Hydrogen-Bonded Mesogens Derived from Alkylpyridines and Benzoic Acids. *Chem. Mater.* **1995**, *7*, 368−372.
(114) Arleth, L.; Xia, X.; Hjelm, R. P.; Wu, J.; Hu, Z. Volume transition and internal structures of small poly(N-isopropylacrylamide) microgels. *J. Polym. Sci., Part B: Polym. Phys.* **2005**, *43*, 849−860.
(115) Miura, M.; Cole, C. A.; Monji, N.; Hoffman, A. S. Temperature-Dependent Absorption/Desorption Behavior of Lower Critical Solution Temperature (LCST) Polymers on Various Substrates. *J. Biomater. Sci., Polym. Ed.* **1994**, *5* (6), 555−568.
(116) Reddy, P. M.; Chang, C.-J.; Hsieh, S.-R.; Huang, H.-C.; Lee, M.-C. Overview of the effect of monomers and green solvents on thermoresponsive copolymers: phase transition temperature and surface properties. *RSC Adv.* **2015**, *5*, 86901−86909.
(117) Da Costa, L. M.; Stoyanov, S. R.; Gusarov, S.; Tan, X.; Gray, M. R.; Stryker, J. M.; Tykwinski, R.; de M. Carneiro, J. W.; Seidl, P. R.; Kovalenko, A. Density functional theory investigation of the contributions of $\pi-\pi$ stacking and hydrogen-bonding interactions to the aggregation of model asphaltene compounds. *Energy Fuels* **2012**, *26*, 2727−2735.
(118) Gawrys, K. L.; Blankenship, G. A.; Kilpatrick, P. K. On the distribution of chemical properties and aggregation of solubility fractions in asphaltenes. *Energy Fuels* **2006**, *20*, 705−714.
(119) Gray, M. R.; Tykwinski, R. R.; Stryker, J. M.; Tan, X. Supramolecular Assembly Model for Aggregation of Petroleum Asphaltenes. *Energy Fuels* **2011**, *25*, 3125−3134.

DOI: 10.1021/acs.energyfuels.9b00600
Energy Fuels 2019, 33, 6934−6945